Cathodoluminescence as a Means for Distinguishing Hydrothermal from Pre-hydrothermal Quartz in Sulfide-Bearing Mineral Deposits on the Northern Fringe of the Upper Mississippi Valley Zinc-Lead District, NE Iowa and SW Wisconsin

Paul L. Garvin
Cornell College

Let us know how access to this document benefits you

Cathodoluminescence as a Means for Distinguishing Hydrothermal from Pre-hydrothermal Quartz in Sulfide-Bearing Mineral Deposits on the Northern Fringe of the Upper Mississippi Valley Zinc-Lead District, NE Iowa and SW Wisconsin

PAUL L. GARVIN

Department of Geology, Cornell College, Mount Vernon, Iowa 52314

Sulfide-bearing mineral deposits, located on the northern fringe of the Upper Mississippi Valley Zinc-Lead District, are contained in early Ordovician carbonate rocks that are extensively silicified and dolomitized. Some silica and dolomite appear to be products of the hydrothermal processes that also formed fracture-filling and cavity-lining sulfides and other cogenetic minerals; other silica and dolomite appear to result from low-temperature, pre-hydrothermal regional diagenesis. Distinguishing hydrothermal quartz (jasperoid) from pre-hydrothermal quartz (chert) solely by hand specimen and thin section petrography is difficult because these two types of mineralization are often intimately associated with each other. Polished slabs from several of these deposits were studied using cathodoluminescence (CL). Demonstrable chert exhibits light to dark blue CL, while demonstrable jasperoid exhibits red-brown to tan CL. It appears that intimately-associated jasperoid and chert can be distinguished with CL. A result is that much of what was previously described as jasperoid in the Upper Mississippi Valley Zn-Pb District is very likely non-hydrothermal chert.

INDEX DESCRIPTORS: cathodoluminescence, quartz, Upper Mississippi Valley Zinc-Lead District.

The Upper Mississippi Valley Zinc-Lead District (UMV) has been studied extensively during the last half century, with recent efforts focusing on hydrothermal fluid dynamics and the sources of metals, sulfur and oxygen. However, since the landmark study by Heyl et al. (1959), little has been reported concerning the nature and distribution of wall rock alteration associated with UMV mineralization. The report of prominent silicification in the northern part of the district, to the extent of wholescale replacement of some dolomite layers (Heyl et al. 1959), has been questioned on the basis of petrographic evidence (Garvin 1982). The close spatial association of hydrothermal quartz (jasperoid) and pre-hydrothermal quartz (chert) makes it difficult to determine the extent of hydrothermal silicification by petrography alone.

The purpose of this study is to investigate the utility of cathodoluminescence, in combination with hand specimen and thin section petrography, as a means for distinguishing hydrothermal jasperoid from pre-hydrothermal chert in UMV deposits. Mineral deposits and their host rocks in the northern fringe of the UMV District (northeastern Iowa and west-central Wisconsin) were selected for this study because hydrothermal silicification is reported to be extensive there (Heyl et al. 1959). These deposits are exposed at the Mineral Creek, Lansing, Plum Creek and Demby-Weist mines (Fig. 1). Comparisons with petrographic observations of other mineralized occurrences in the northern fringe (e.g., Copper Creek Mine, Bridgeport Quarry, Mount Sterling Quarry) indicate that hydrothermal alteration throughout the area is broadly similar.

GENERAL GEOLOGY AND DESCRIPTIONS OF THE MINERAL DEPOSITS

The four mineral deposits of this study are hosted by the Oneota Formation of early Ordovician (Tremadocian) age (Fig. 2). The Oneo-

ta is divided into two members, the Stockton Hill and the overlying Hager City. Descriptions of these units are given by Ludvigson (1976). In brief, the Stockton Hill is a dolomitic quartz sandstone. Its composition ranges from nearly pure quartz to nearly pure dolomite. It contains ooliths, algal stromatolites, intraclasts, chert and glauconite (Ludvigson 1976). The Hager City is a medium crystalline saccharoidal dolomite, containing minor chert and shale. Primary structures are poorly preserved. Vugs lined with calcite crystals and/or drusy quartz are commonly observed on a regional basis.
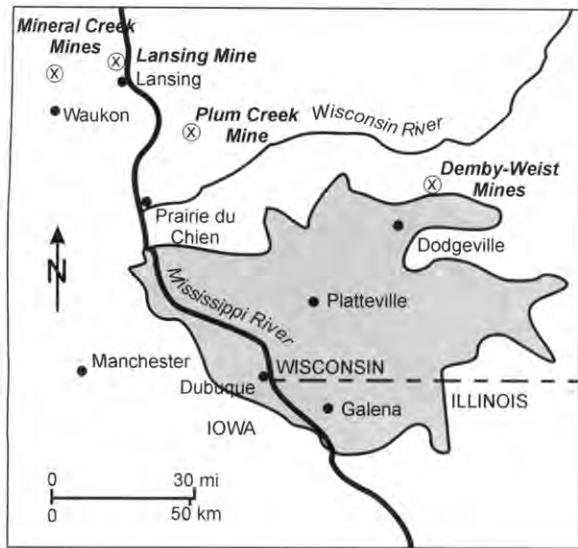
Detailed descriptions of the four deposits are given in Heyl et al. (1959), Ludvigson (1976), Garvin (1982) Heyl et al. (1982) and Garvin et al. (1987). All primary sulfide minerals have been variably altered to oxidized species. Summary descriptions follow.

Mineral Creek Mines

The Mineral Creek Mines are located in central Allamakee County, Iowa (Fig. 1). The mineralization is hosted by dolomite of the Oneota Formation and is contained in northeast-trending fold-associated extensional fractures, and in areas of collapse breccia that are scattered along the fold crest (Fig. 3). Primary vein-filling and cavity-lining minerals are marcasite (FeS_2), pyrite (FeS_2), galena (PbS), sphalerite (ZnS) and calcite ($CaCO_3$).

Lansing Mine

The Lansing Mine is located in eastern Allamakee County, Iowa (Fig. 1). Mineralization is contained within a north-trending vertical fracture ("gash vein") in the Oneota Formation, which extends downward into the underlying Jordan Sandstone (Fig. 3). Primary minerals are quartz, pyrite, marcasite, galena, and sphalerite, with minor calcite.

Fig. 1. Map showing locations of mineral deposits used in this study.

Fig. 2. Stratigraphic section of Cambrian and Ordovician host rocks for mineral deposits in this study. Modified from Heyl et al. (1959), with additional data from Ludvigson (1976).

Demby-Weist Mines

The Demby-Weist Mines are located in northern Iowa County, Wisconsin (Fig. 1). Mineralization is contained within vertical northwest-trending *en echelon* fractures in the Oneota Formation, which extend downward into the Jordan Sandstone (Fig. 3). Primary minerals are marcasite, pyrite, galena and sphalerite.

Plum Creek Mine

The Plum Creek Mine is located in central Crawford County, Wisconsin (Fig. 1). Mineralization is contained in fold-controlled paleokarst depressions in the Oneota Formation near its contact with the overlying St. Peter Sandstone (Fig. 3). Primary minerals are pyrite, marcasite, chalcopyrite and minor calcite.

PETROGRAPHIC ANALYSIS OF HOST ROCK DOLOMITE AND QUARTZ

The mineralogy of the host rocks for all four deposits consists of dolomite, quartz, and rare celadonite.

Dolomite

Regional diagenetic (low temperature, pre-hydrothermal) and hydrothermal dolomite are abundant in the Oneota Formation in areas where it is mineralized (Smith et al. 1996). The most reliable criteria for distinguishing between the two types of dolomite are crystal size and presence or absence of crystal zoning. Hydrothermal dolomite is relatively coarse, and crystals are commonly euhedral and zoned, especially where they line dissolution cavities or are scattered in quartz (Figs. 4a, b). Zoning is especially prominent at the Demby-Weist and Plum Creek Mines. Aggregations of coarse hydrothermal dolomite in a matrix of fine, equigranular regional dolomite occur locally, resulting in a somewhat mottled texture.

Quartz

Quartz is also abundant in the Oneota Formation, as pre-hydrothermal chert and hydrothermal jasperoid. Based on crystal habit five types are recognized (Neybert and Garvin 1979): cryptocrystalline (C), microcrystalline (M), fibrous (chalcedonic) (F), drusy (D) and detrital (T).

C-quartz occurs as pseudomorphic replacements of oolitic, peloidal and skeletal grains and of matrix in the original carbonate rock (Figs. 4c, d, g, and i). It also appears as irregular, structureless masses (Figs. 4g, h). Optically it is nearly isotropic and may contain minute fluid inclusions or solid impurities. It appears more or less chalky due to dissolution and replacement by dolomite.

M-quartz replaces carbonate matrix, fossil shells (particularly brachiopods and gastropods) and locally, ooliths, and it lines dissolution cavities and open fractures (Figs. 4c, d, e, f, g). Locally it occurs as irregular patches in C-quartz. M-quartz grades into C-quartz and D-quartz. Where lining open cavities it generally coarsens inward to D-quartz.

F-quartz exhibits typical banded, colloform and locally spherulitic habit (Fig. 4f). It may display what appear to be shrinkage cracks, suggesting colloidal origin. It is interlayered with M-quartz in cavity fillings and occurs as islands in dolomite. Locally it forms narrow bands within, and lines interstices between, silicified ooliths, which were later filled with M-quartz.

D-quartz lines or fills dissolution cavities or open fractures (Fig. 4h). It is commonly banded, a consequence of changes in crystal size and color during deposition. It stands out as fresh veinlets in chalky C-quartz. It commonly lines or fills cavities that were previously
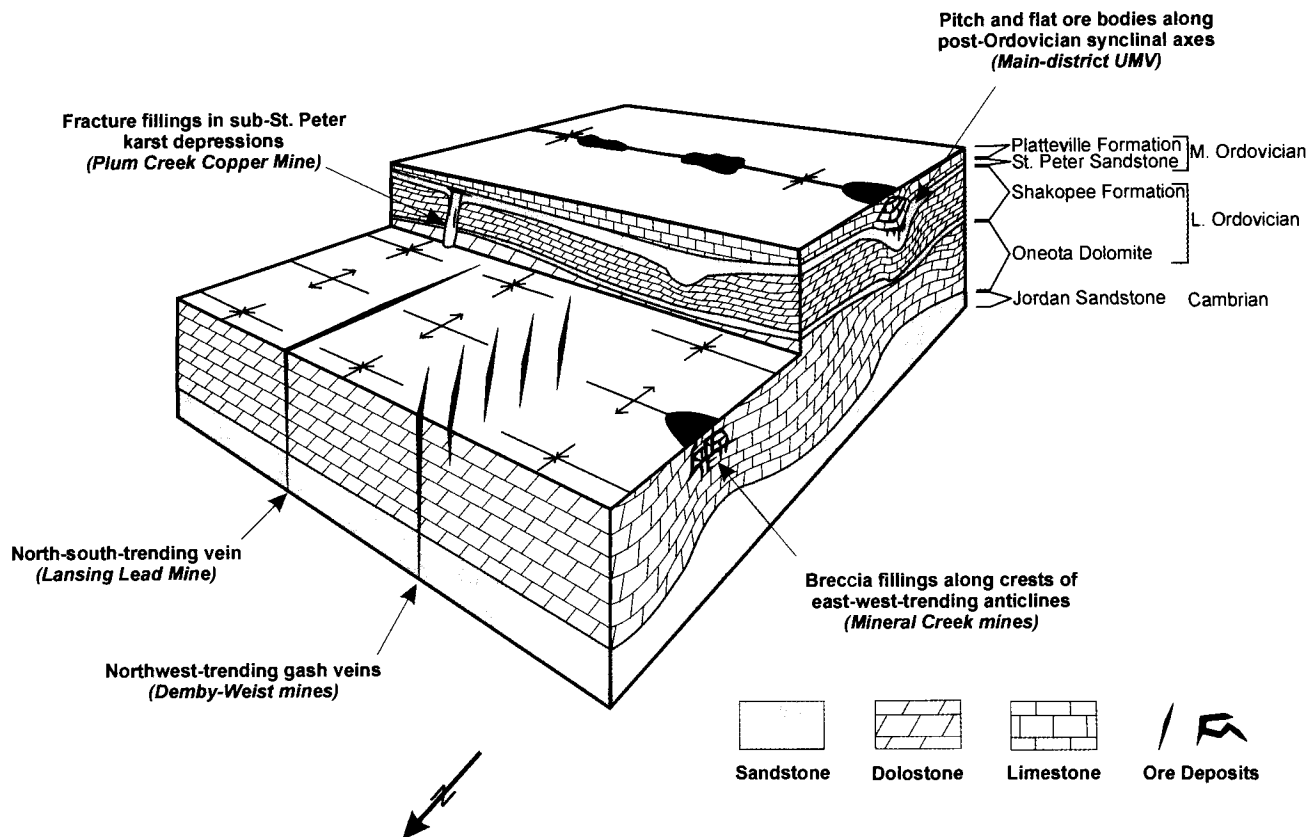
Fig. 3.   Block diagram showing structural and stratigraphic controls on distribution of mineral deposits in this study. Modified from Ludvigson et al. (1983).

lined with F-quartz. It is especially abundant at the Lansing and Demby-Weist mines. D-quartz is gradational with M-quartz. At the Plum Creek and Demby-Weist mines D-quartz is locally pink to red, probably due to the presence of sub-microscopic inclusions of hematite.

T-quartz occurs as nuclei of ooliths or is interstitial to them (Fig. 4i). In both cases detrital grains are sub-rounded to well-rounded. It is a minor constituent in all of the deposits studied, except Lansing.

PETROGRAPHIC ANALYSIS OF QUARTZ

Detailed petrographic analysis of the interrelationships among the varieties of quartz and their relationships to dolomite in Prairie du Chien host rocks reveals that much quartz, perhaps the greatest amount in volumetric terms, was deposited prior to the onset of hydrothermal activity. This observation applies to all T-quartz and C-quartz, and much of the M-quartz and F-quartz. Evidences for the pre-hydrothermal origin of this quartz are: 1) C-quartz and some M-quartz occur in what appear to be chert nodules, having typical smooth, sharp contacts with dolomite. Nodule boundaries are locally corroded because of replacement by dolomite. The fine-grained nature of, and the absence of zoned euhedral crystals in, the replacing dolomite indicate that it is also regional diagenetic and pre-hydrothermal (Garvin 1982). Nodular chert and pervasive dolomite are typical of unmineralized Oneota Formation. 2) C-quartz and M-quartz frequently replace ooliths and peloids. Preservation of fine-scale concentric banding in ooliths is common. Ooliths are rare in adjacent dolomite and, where present, are poorly preserved. Preser-

vation of ooliths indicates that C- and M-quartz preceded pre-hydrothermal dolomitization. 3) Fossil remains, like ooliths and peloids, are restricted to areas of C-quartz and M-quartz, a further indication that this quartz formed before pre-hydrothermal dolomitization. 4) Breccia clasts in solution-collapse pockets contain C-quartz, M-quartz and F-quartz. This silicification clearly predates collapse, which predates hydrothermal activity. 5) F-quartz islands in dolomite have embayed boundaries and otherwise show evidence of replacement by pre-hydrothermal dolomite. 6) The chalky nature of much of the C-quartz is due to dissolution and partial replacement by pre-hydrothermal dolomite.

Based on hand specimen and thin section petrography, all D-quartz and coeval M-quartz and F-quartz appear to be hydrothermal; all other quartz is pre-hydrothermal. Hydrothermal quartz occurs in fractures and vugs that cut across preexisting C, M and F quartz. It is also found in open fractures and vugs in dolomite. In some openings mineral sulfides are found directly upon D-quartz linings. The possibility of hydrothermal remobilization of some pre-hydrothermal C, M and F quartz cannot be ruled out.

QUARTZ CATHODOLUMINESCENCE

General Considerations

Cathodoluminescence is observed when a substance is irradiated, while under vacuum, with a beam of electrons. Excitation of electrons in the substance and their subsequent return to ground-state energy levels cause selective absorption of visible light. The trapping of electrons in excited states requires defects in the crystal lattice and/or the presence of so-called impurity activator elements, notably
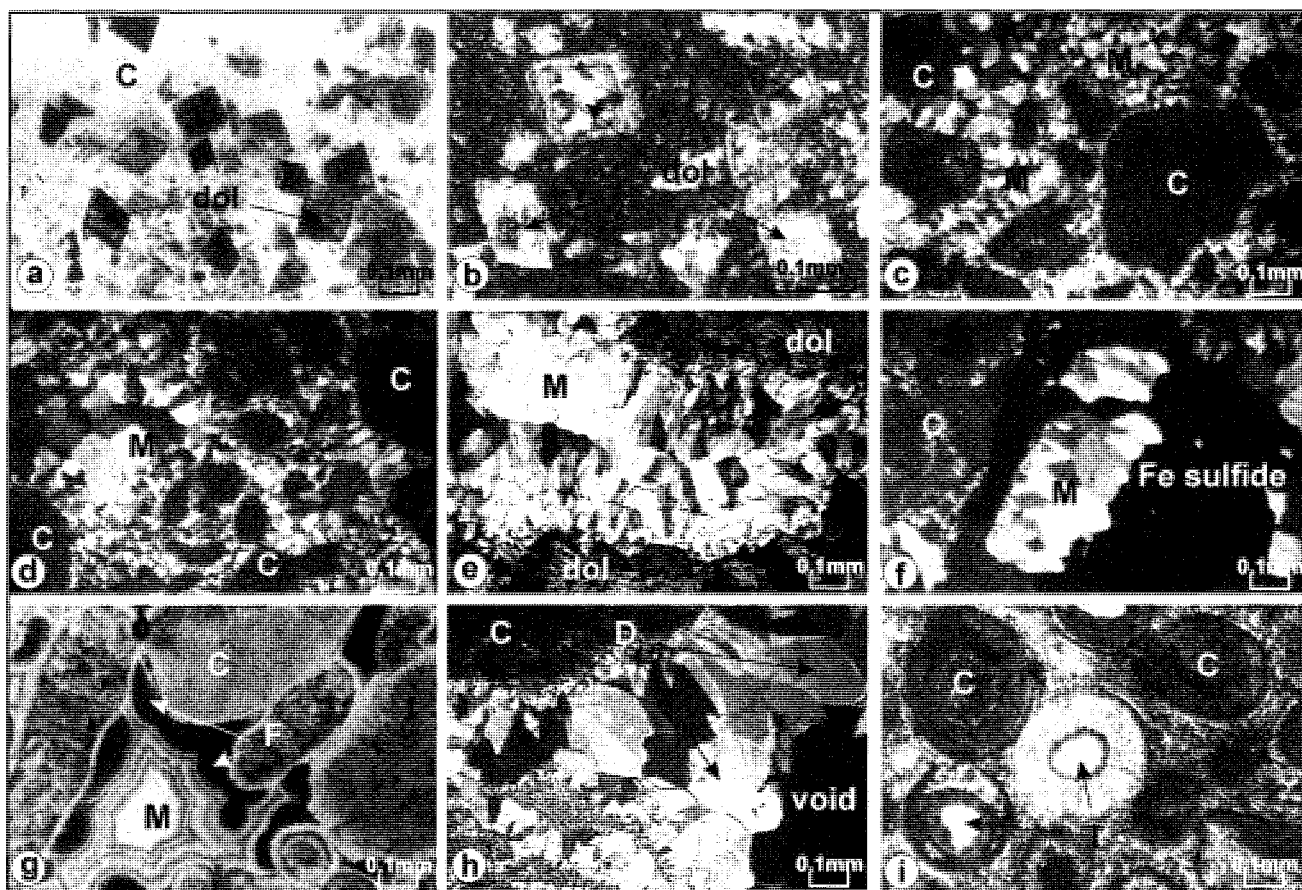
Fig. 4. Photomicrographs of thin sections showing quartz types and quartz-dolomite relations. Abbreviations: C = cryptocrystalline quartz; M = microcrystalline quartz; F = fibrous quartz; D = drusy quartz; T = detrital quartz; dol = dolomite; mine names given in parentheses. *a*: euhedral dolomite replacing cryptocrystalline quartz (Demby-Weist); *b*: zoned euhedral dolomite (Demby-Weist); *c* and *d*: peloids replaced by cryptocrystalline quartz with microcrystalline quartz pore fillings (Lansing); *e*: microcrystalline fracture filling in dolomite (Plum Creek); *f*: cryptocrystalline and microcrystalline quartz engulfed by Fe-sulfide (Lansing); *g*: peloids replaced by cryptocrystalline quartz with microcrystalline and fibrous quartz pore fillings (Mineral Creek); *h*: cryptocrystalline quartz containing vug lined with drusy quartz (Demby-Weist); *i*: ooliths, some with detrital quartz nuclei, replaced by cryptocrystalline quartz; note concentric banding (Demby-Weist).

transition metals, lanthanides and actinides. In a crystal lattice these elements experience crystal field splitting, the magnitude of which is influenced by characteristics of the crystal structure (e.g., bond type, coordination number) and the valence of the impurity element. Certain elements called quenchers (e.g. Fe^{2+}, Fe^{3+}, Co^{2+}, Ni^{2+}) reduce crystal field splitting and, in turn, reduce the intensity of luminescence (Ramseyer and Mullis 2000).

Cathodoluminescence (CL) in quartz has been investigated extensively (Hagni 1987, Marshall 1988, Ramseyer and Mullis 2000). Quartz CL has proven to be particularly useful in sedimentological studies (for example to distinguish detrital quartz from diagenetic or metamorphic overgrowths [Smith and Stenstrom 1965, Sippel 1968, Grant and White 1978, Krinsley and Tovey 1978, Bruhn et al. 1996, Demars et al. 1996, Tennison et al. 2001], and to determine provenance of quartz in sandstone and mudrocks [Milliken 1994, Seyedolali et al. 1997, Walderhaug and Rykkje 2000, Boggs et al. 2002, Kwon and Boggs 2002]), in studies of magmatic and hydrothermal systems (Graupner et al. 2000, Müller 2000, Penniston-Dorland 2001, Peppard et al. 2001, Rusk and Reed 2002), in studies of diagenesis (Walker and Burley 1991, Goetze et al. 1999), radiation damage (Owen 1988) and in identification of shock meta-

morphism (Owen and Anders 1988, Seyedolali et al. 1996, Boggs et al. 2001).

Spectral CL colors in α-quartz are dominantly shades of red and blue. The origin of CL coloration has received considerable attention, but is still not well understood. Bruhn et al. (1996) attempted to correlate quartz CL color with trace element composition of detrital grains and diagenetic cement in sandstones. They found that orange-brown cement had a relatively high content of Fe (up to 192 ppm), whereas in non-luminescing cement the Fe content was significantly lower. They also discovered that red-brown detrital grains had a relatively high Fe content (up to 455 ppm), while violet-blue grains had a relatively high content of Ti (up to 298 ppm). Red CL emission might be due to substitutional incorporation of Fe^{3+} in the quartz lattice (Sprunt 1981, Müller 2000) or Mn^{2+} (Claffy and Ginther 1959, Nickel 1978). Substitution of Fe for Si increases with an increase in temperature of formation. Thus hydrothermal quartz might show more red CL than quartz formed at lower temperature (Müller 2000). This interpretation is equivocal, because it is well established that blue-luminescing quartz also forms under magmatic conditions. Quartz CL color may vary with crystallographic orientation (Walderhaug and Rykkje 2000).
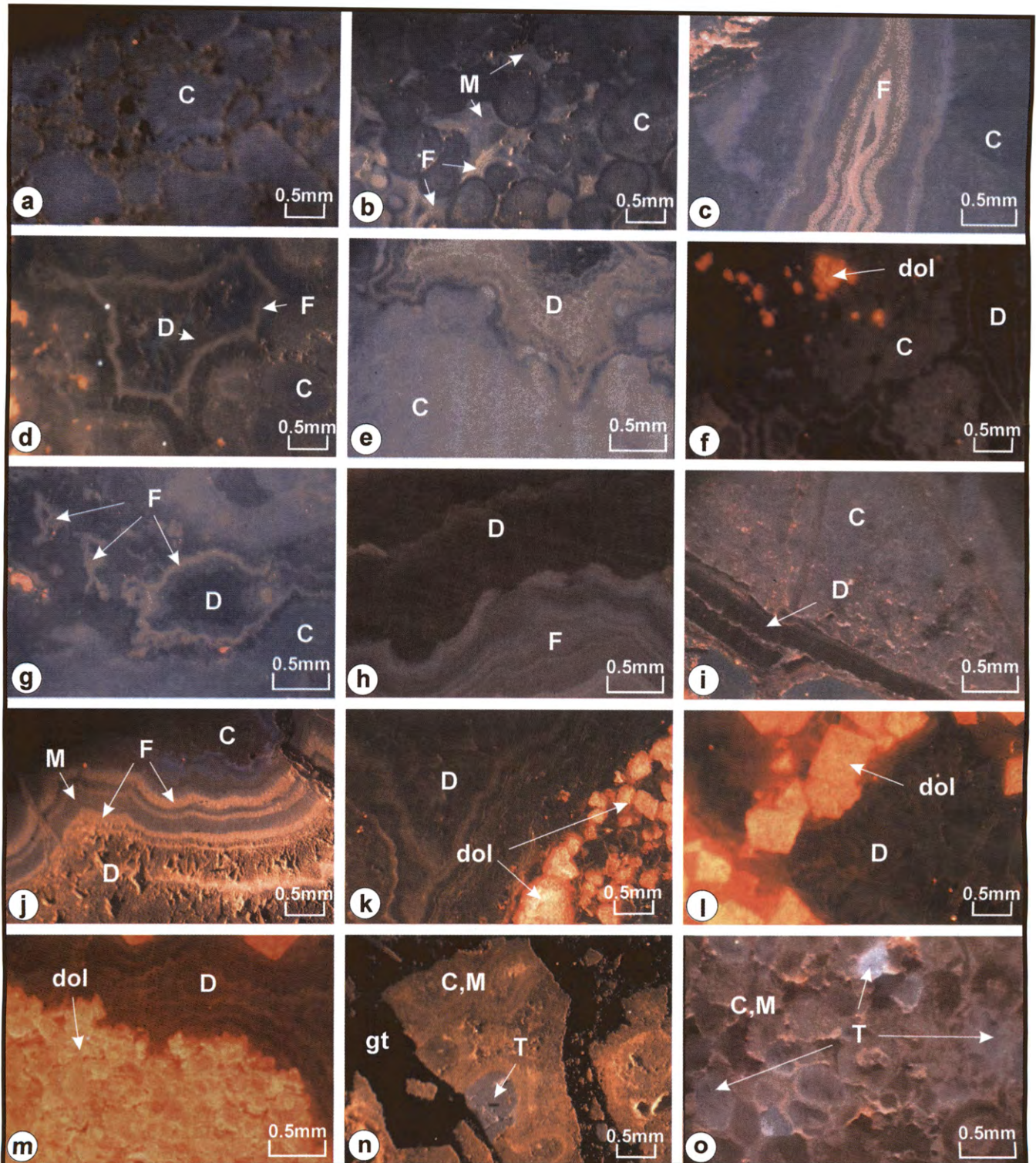
Fig. 5. Photomicrographs of polished slabs showing differences in cathodoluminescence colors for different types of quartz. Abbreviations: C = cryptocrystalline quartz; M = microcrystalline quartz; F = fibrous quartz; D = drusy quartz; T = detrital quartz; dol = dolomite; gt: goethite (altered Fe-sulfide); mine names given in parentheses. *a*: peloids replaced by cryptocrystalline quartz (Lansing); *b*: peloids replaced by crypto-crystalline quartz with pore fillings of microcrystalline quartz; some alteration of original blue CL color to tan (Plum Creek); *c*: cryptocrystalline quartz with fracture filled with fibrous quartz (Lansing); *d*: peloids replaced by cryptocrystalline quartz with pore fillings of fibrous and drusy quartz; some alteration of original blue CL color (Plum Creek); *e*: cryptocrystalline quartz containing vug lined with drusy quartz; some alteration of original blue CL color (Plum Creek); *f*: cryptocrystalline quartz containing vugs lined with drusy quartz; some dolomite replacement; some alteration of original blue CL color (Demby-Weist); *g*: cryptocrystalline quartz containing vugs lined with fibrous and drusy quartz; some

The blue CL color in some varieties of quartz alters irreversibly to varying shades of brown during irradiation of the sample by the electron beam. In some cases intermittent flashes of blue light are observed, in others the change is gradual, though quite rapid (a few minutes or less). The unstable blue color appears to correlate with high Al $^{3+}$ content (Ramseyer and Mullis 1990); and possibly Li $^+$ or Na $^+$, which compensate for the substitution of Al $^{3+}$ for Si $^{4+}$ (Perney et al. 1992). The rate of blue CL alteration is influenced by electron beam voltage and the amount of beam focusing. A thorough treatment of the causes of CL color in quartz is given by Müller (2000).

Methods

Observations of quartz CL were made using a Nuclide ELM-2E luminoscope, with the viewing chamber mounted on a standard petrographic microscope. Alteration of initial color of blue-luminescing quartz during exposure to the electron beam was rapid, particularly with fine-grained C-quartz and F-quartz (less than two minutes). Efforts were made to reduce the rate of blue-color alteration and the time of exposure of the sample to the beam, while at the same time providing sufficient light to the camera film, which is necessitated by the low intensity of quartz CL. The rate of alteration was slowed substantially by means of the following procedures. 1) Polished slabs (2–7 mm thick) were used in order to dissipate heat more effectively. 2) The operating voltage and beam current were kept as low as possible (10 kV, 0.1 to 0.2 mA, respectively). 3) An unfocused beam was used. Film exposure concerns were addressed as follows. 1) A low power objective lens (3.5x) was used to increase the amount of light received by the microscope and the camera lens, hence to decrease the exposure time. 2) A film with a high ISO rating was used. 3) The film was push processed in order to increase the effective ISO. Best results in terms of color fidelity and resolution were obtained with 3M Color 1000, push-processed to ISO 1600. Exposure times ranged from 30 to 240 seconds.

Results and Interpretations

The results described here are generalizations for all four deposits. There is great uniformity among the deposits.

1. *D-quartz and associated M-quartz and F-quartz.* Initial CL colors range from dark to light brown. Lighter colors are restricted to more finely crystalline bands. Colors do not change during irradiation (Figs. 5d, e, f, g, h, i, j, k, l, m).
2. *C-quartz and associated M-quartz.* Initial CL colors are generally blue. Structureless isotropic varieties are dark blue and are seen where the petrography indicates a chert nodule (Figs. 5c, e, f, g, i). Colors change during irradiation to purple, then brown. C-quartz and M-quartz CL colors in silicified ooliths are initially blue, except where the ooliths contain visible impregnations of iron oxide, as at Demby-Weist (Figs. 5a, b, d, o). Here, initial CL colors are brown to red-brown. Iron oxide appears to have been introduced during weathering. Locally, where C-quartz is

Table 1. Initial and post-irradiation cathodoluminescent colors for different varieties of quartz.

Quartz Type[a]	Prehydrothermal/ Hydrothermal	Initial CL Colors	Postirradiation CL Colors
C	Prehydrothermal	Dark to medium blue	Brown
M/C	Prehydrothermal	Blue	Brown
F/C	Prehydrothermal	Light to medium blue	Tan to orange tan
T	Prehydrothermal	Medium blue	Same as initial
D	Hydrothermal	Dark to light brown	Same as initial
M/D	Hydrothermal	Dark to light brown	Same as initial
F/D	Hydrothermal	Orange brown to tan	Same as initial

[a] C = cryptocrystalline quartz; M/C = microcrystalline quartz in association with cryptocrystalline quartz; D = drusy quartz; F/C = fibrous quartz in association with cryptocrystalline quartz; F/D = fibrous quartz in asociation with drusy quartz; M/D = microcrystalline quartz in association with drusy quartz; T = detrital quartz.

invaded by D-quartz, there appears to be a brown CL halo extending a fraction of a millimeter into the blue C-quartz (Figs. 5e, g). Elsewhere, the contact between the two is sharp.

3. *F-Quartz.* F-quartz is of two types. For F-quartz that is coeval with C-quartz, the initial CL colors range from relatively intense light to medium blue (Fig. 5h). This type exhibits concentric banding and occurs as islands in C-quartz or dolomite. It is also interstitial to ooliths. During irradiation, CL colors change quite rapidly to purple, tan, and finally orange-tan. At high beam current the color change goes to completion in a very few minutes and is permanent. For F-quartz that is coeval with D-quartz, initial CL colors are orange-brown to tan (Figs. 5d, j). The best examples come from the Lansing Mine. Brown-luminescing F-quartz remains brown during irradiation.

4. *T-quartz.* Initial color of detrital quartz grains is medium blue. Color change does not occur during irradiation; hence, the contrast between detrital quartz and adjacent silicified ooliths becomes progressive greater during irradiation as the ooliths turn brown (Figs. 5n, o).

See Table 1 for comparisons of initial and post-irradiation CL colors for the different varieties of quartz.

In the absence of trace element and crystal structure analyses, the causes of CL coloration in quartz from the four deposits cannot be determined with certainty. Based on other studies, initial brown luminescence may indicate the presence of substituent Fe $^{3+}$ in the

←

alteration of original blue CL color (Mineral Creek); *h*: drusy quartz-filled fracture in fibrous quartz; significant alteration of original blue CL color (Lansing); *i*: drusy quartz-filled fracture in cryptocrystalline quartz; significant alteration of original blue CL color (Plum Creek); *j*: cryptocrystalline quartz with fracture lined with fibrous and drusy quartz; some alteration of original blue CL color (Lansing); *k*: dolomite containing vug lined with drusy quartz (Plum Creek); *l*: euhedral dolomite rhombs and drusy quartz (Demby-Weist); *m*: dolomite with drusy quartz vein (Plum Creek); *n*: breccia, consisting of ooliths replaced by cryptocrystalline quartz with microcrystalline quartz pore fillings; detrital quartz quartz nucleus; breccia cement is goetite (altered Fe-sulfide); strong alteration of original blue CL color in cryptocrystalline and microcrystalline quartz, but no alteration in detrital quartz (Plum Creek); *o*: peloids replaced by cryptocrystalline quartz and detrital quartz grains, with pore fillings of microcrystalline quartz; significant alteration of original blue CL coloration in cryptocrystalline and microcrystalline quartz, but no alteration in detrital quartz (Plum Creek).

quartz lattice (Bruhn et al. 1996), while unstable blue luminescence may indicate the presence of substituent Al $^{3+}$, along with compensating Na $^{+}$ or Li $^{+}$ in the lattice (Perney et al. 2000).

CONCLUSIONS

Initial CL colors of the several varieties of quartz occurring in the Oneota Dolomite, supported by petrographic evidence, indicate three different origins of quartz: 1) Medium blue-luminescing detrital quartz grains, presumably derived from Precambrian crystalline rock, were transported into an Ordovician depositional basin, where they became nuclei for oolith formation. 2) Dark- to medium-blue-luminescing cryptocrystalline, microcrystalline, and fibrous quartz (pre-hydrothermal chert and chalcedony) appear to have originated by the diagenetic replacement of limestone prior to regional dolomitization. 3) Brown-luminescing drusy, microcrystalline, and fibrous quartz (hydrothermal jasperoid), which are localized as vein fillings and small cavity linings, were probably introduced into the chert-bearing Oneota Dolomite during early stages of hydrothermal activity, probably during the late Paleozoic.

Volumetrically, chert is far more abundant than jasperoid in these deposits. Thus, hydrothermal silicification, while pervasive, is not as prominent as earlier reported (Heyl et al. 1959).

It appears that cathodoluminescence can be a useful tool for distinguishing hydrothermal from non-hydrothermal quartz in carbonate-hosted zinc-lead deposits.

ACKNOWLEDGMENTS

LITERATURE CITED

BOGGS, S., Jr., Y-I KWON, G. G. GOLES, B. G. RUSK, D. KRINSLEY, and A. SEYEDOLALI. 2002. Is quartz cathodoluminescence color a reliable provenance tool? A quantitative examination: Journal of Sedimentary Research 72: 408–415.

BOGGS, S., Jr., D. H. KRINSLEY, G. G. GOLES, A. SEYEDOLALI, and H. DYPVIK. 2001. Identification of shocked quartz by scanning cathodoluminescence imaging. Meteoritics and Planetary Science 36:783–792.

BRUHN, F., P. BRUCKSHEN, J. MEIJER, A. STEPHAN, D. K. RICHTER, and J. VEIZER. 1996. Cathodoluminescence investigations and trace element analysis of quartz by micro-PIXE: implications for diagenetic and provenance studies in sandstone. Canadian Mineralogist 34: 1223–1232.

CLAFFY, E. W., and R. J. GINTHER. 1959. Red-luminescing quartz. American Mineralogist 44:987–994.

DEMARS, C., M. PAGEL, E. DELOULE, and P. BLANC. 1996. Cathodoluminescence of quartz from sandstones: Interpretation of the UV range by determination of trace element distributions and fluid inclusion P-T-X properties in authigenic quartz. American Mineralogist 81:891–901.

GARVIN, P. L. 1982. Sulfide mineralization at Mineral Creek Mines, Allamakee County, Iowa: Iowa Academy of Science Proceedings 90:44–49.

GARVIN, P. L., G. A. LUDVIGSON, and E. M. RIPLEY. 1987. Sulfur isotope reconnaissance of minor metal sulfide deposits fringing the upper Mississippi Valley Zinc-Lead District. Economic Geology 82:1386–1394

GOETZE, J., M. PLOETZE, H. FUCHS, and D. HABERMANN. 1999. Defect structures and luminescence behaviour of agate: results of electron paramagnetic resonance (EPR) and a cathodoluminescence (CL) studies: Mineralogy Magazine 63:149–163.

GRANT, P. R., and S. H. WHITE. 1978. Cathodoluminescence and microstructure of quartz overgrowths on quartz. Scanning Electron Microscopy 1978, part 1:789–793.

GRAUPNER, T., J. GOETZE, U. KEMPE, and D. WOLF. 2000. CL for characterizing quartz and trapped fluid inclusions in mesothermal quartz veins: Muruntau Au ore deposit, Uzbekistan: Mineralogical Magazine 64: 1007–1016.

HAGNI, R. D. 1987. Industrial applications of cathodoluminescence microscopy. Pages 37–52. In Process mineralogy IV: Applications to precious metal deposits, industrial minerals, coal, liberation, mineral processing, agglomeration, metallurgical products, and refractories, with special emphasis on cathodoluminescence microscopy. R. D. Hagni (ed.). TMS, Warrendale, Pennsylvania.

HEYL, A. V., A. F. AGNEW, E. J. LYONS, and C. H. BEHRE. 1959. The geology of the Upper Mississippi Valley Zinc-Lead District. United States Geologic Survey Professional Paper 309. 310p.

HEYL, A. V., and W. S. WEST. 1982. Outlying mineral occurrences related to the Upper Mississippi Valley mineral district, Wisconsin, Iowa, Illinois and Minnesota: Economic Geology 77:1803–1817.

KRINSLEY, D. H., and N. K. TOVEY. 1978. Cathodoluminescence in quartz sand grains. Scanning Electron Microscopy; International Review of Advancements in Technological Applications of Scanning Electron Microscopy 1978, part 1:887–892.

KWON, Y-I., and S. BOGGS. 2002. Provenance interpretation of Tertiary sandstones from the Cheju Basin (NE East China Sea): A comparison of conventional petrographic and scanning cathodoluminescence techniques. Sedimentary Geology 152:29–43.

LUDVIGSON, G. A. 1976. LANDSAT-1 identified linears in northeast Iowa and Southwest Wisconsin and their relation to the Ordovician sttatigraphy, structure, and sulfide mineralization in the area. Unpublished MS Thesis, University of Iowa. 196p.

LUDVIGSON, G. A., B. J. BUNKER, B. J. WITZKE, and P. L. GARVIN. 1983. A burial diagenetic model for the emplacement of zinc-lead sulfide ores in the upper Mississippi Valley, U.S.A. Pages 497–515. In Proceedings of the International Conference on Mississippi Valley-Type lead-zinc deposits, G. Kisvarsanyi, S. K. Grant, W. P. Pratt, and J. W. Koenig (eds.). University of Missouri-Rolla, Rolla, Missouri.

MARSHALL, D. J. 1988. The cathodoluminescence of quartz and some geological applications. Pages 67–91. In Cathodoluminescence of geological materials. Unwin Hyman. 146p.

MILLIKEN, K. L. 1994. Cathodoluminescence textures and the origin of quartz silt in Oligocene mudrocks, South Texas: Journal of Sedimentary Research 64:567–571.

MÜLLER, A. 2000. Cathodoluminescence and characterization of defect structures in quartz with applications to the study of granitic rocks. Ph. D. Dissertation, University of Göttingen. Retrieved 2002, Oct 10 from: http://webdoc.gwdg.de/diss/2001/mueller/diss.pdf

NEYBERT, D. F., and P. L. GARVIN. 1979. Petrographic analysis of wallrock alteration in Prairie du Chien-hosted lead-zinc deposits in northeastern Iowa and southwestern Wisconsin. unpublished data, Cornell College.

NICKEL, E. 1978. The present status of cathode luminescence as a tool in Sedimentology. Minerals Science and Engineering 10:73–100.

OWEN M.R. 1988. Radiation-damage halos in quartz: Geology 16:529–532.

OWEN, M. R., and M. H. ANDERS. 1988. Evidence from cathodoluminescence for non-volcanic origin of shocked quartz at the Cretaceous/Tertiary boundary: Nature 334:145–147.

PENNISTON-DORLAND, S. C. 2001. Illumination of vein quartz textures in a porphyry copper deposit using scanned cathodoluminescence: Grosburg Igneous Complex, Irian Java, Indonesia: American Mineralogist 86: 652–686.

PEPPARD, B. T., J. M. STEELE, A. M. DAVIS, P. J. WALLACE, and A. T. ANDERSON. 2001. Zoned quartz phenocrysts from the rhyolitic Bishop Tuff: American Mineralogist 86:1034–1052.

PERNEY, B., P. EBERHARDT, K. RAMSEYER, J. MULLIS, and R. PANKRATH. 1992. Microdistribution of Al, Li, and Na in α-quartz: Possible causes and correlation with short-lived cathodoluminescence. American Mineralogist 77:534–544.

RAMSEYER, K., and J. MULLIS. 1990. Factors influencing short-lived blue cathodoluminescence of α-quartz. American Mineralogist 75:791–800.

RAMSEYER, K., AND J. MULLIS. 2000. Geological application of cath-

odoluminescence of silicates. Pages 177–191. *In* Cathodoluminescence in geosciences. M. Pagel, V. Barbin, P. Blanc, and D. Ohnenstetter (eds.) Springer-Verlag, Berlin.

RUSK, B., and M. REED. 2002. Scanning electron microscope-cathodoluminescence analysis of quartz reveals complex growth in veins from the Butte porphyry copper deposit, Montana: Geology 30:727–730.

SEYEDOLALI, A., D. KRINSLEY, G. J. RETALLACK, W.T. HOLSER, and H.DYPVIK. 1996. Identification of shocked quartz from the Permian/Triassic and Jurassic/Cretaceous boundaries using cathodoluminescence: EOS, Transactions, American Geophysical Union 77:777.

SEYEDOLALI, A., D. H. KRINSLEY, S. BOGGS, Jr., P. F. O'HARA, H. DYPVIK, and G. G. GOLES. 1997. Provenance interpretation of quartz by scanning electron microscope-cathodoluminescence fabric analysis: Geology 25:787–790.

SIPPEL, R. F. 1968. Sandstone petrology, evidence from luminescence petrography. Journal of Sedimentary Petrology. 38:530–554.

SMITH, G. L., C. W. BYERS, and R. H. DOTT, Jr. 1996. Sequence stratigraphy of the Prairie du Chien Group, Lower Ordovician, Midconti-

nent, U. S. A. Pages 23–33. *In* Paleozoic Sequence Stratigraphy: Views from the North American Craton, B. J. Witkze, G. A. Ludvigson, and J. Day (eds.). Geological Society of America Special Paper 306.

SMITH, J. V., and R. C. STENSTROM. 1965. Electron-excited luminescence as a petrologic tool. Journal of Geology 73:627–635.

SPRUNT, E. S. 1981. Causes of quartz cathodoluminescence colors. Scanning Electron Microscopy 1:525–535.

TENNISON, E., J. SCHIEBER, and D. KRINSLEY. 2001. Textural features of metamorphic quartz as revealed by scanned cathodoluminescence (SEM-CL): Potential use in provenance studies. Geological Society of America. Abstracts with Programs 33:72.

WALDERHAUG, O., and J. RYKKJE. 2000. Some examples of the effect of crystallographic orientation on the cathodoluminescence colors of quartz: Journal of Sedimentary Research 70:545–548.

WALKER, G., and S. D. BURLEY. 1991. Luminescence petrography and spectroscopic studies of diagenetic minerals. Pages 83–96. *In* Luminescence microscopy and spectroscopy: qualitative and quantitative applications. O. C. Kopp (ed.). Society of Economic Paleontologists and Mineralogists, Short Course Notes 25. Tulsa, Oklahoma.